Physiological Measurement

IPEM Institute of Physics and Engineering in Medicine

PAPER

Noninvasive mapping reveals recurrent and suddenly changing patterns in atrial fibrillation—a magnetocardiographic study

To cite this article: Ville Mäntynen *et al* 2018 *Physiol. Meas.* **39** 025006

View the article online for updates and enhancements.

This content was downloaded from IP address 130.233.140.92 on 26/02/2018 at 12:22

IOP Publishing Physiol. Meas. 39 (2018) 025006 (10pp) https://doi.org/10.1088/1361-6579/aaa3bb

Physiological Measurement

IPEM Institute of Physics and Engineering in Medicine

PAPER

RECEIVED
12 June 2017

REVISED
15 December 2017

ACCEPTED FOR PUBLICATION
22 December 2017

PUBLISHED
26 February 2018

Noninvasive mapping reveals recurrent and suddenly changing patterns in atrial fibrillation—a magnetocardiographic study

Ville Mäntynen[1,2], **Mika Lehto**[1,3], **Hannu Parikka**[1,3] **and Juha Montonen**[1]

[1] BioMag Laboratory, HUS Medical Imaging Center, University of Helsinki and Helsinki University Hospital, PO Box 340, FI-00029 HUS, Finland

[2] Department of Neuroscience and Biomedical Engineering, Aalto University, Espoo, Finland, PO Box 12200, FI-00076 AALTO, Finland

[3] Heart and Lung Center, University of Helsinki and Helsinki University Hospital, PO Box 340, FI-00029 HUS, Finland

E-mail: ville.mantynen@aalto.fi

Keywords: atrial fibrillation, magnetocardiography, noninvasive mapping

Supplementary material for this article is available online

Abstract

Objective: To study noninvasive magnetocardiographic (MCG) mapping of ongoing atrial fibrillation (AF) and, for the possible mapping patterns observed, to develop simplified but meaningful descriptors or parameters, providing a possible basis for future research and clinical use of the mappings. *Approach*: MCG mapping with simultaneous ECG was recorded during arrhythmia in patients representing a range of typical, clinically classical atrial arrhythmias. The recordings were assessed using MCG map animations, and a method to compute magnetic field map orientation (MFO) and its time course was created to facilitate presentation of the findings. All the data were segmented into four categories of ECG waveform regularity. *Main results*: In visual observation of the MCG animations, an abundance of clear spatial and temporal patterns with regularity were found, often perceived as rotations of the map. This rotation and its sudden reversals of direction were distinctly present in the time course of the MFO. The shortest segments with consistent rotation lasted for some hundreds of milliseconds, i.e. a couple of cycles, but segments lasting for tens of seconds were observed as well. In the ECG, all four categories of regularity were present. The rotation of the MFO was observed in all patients under study and regardless of the ECG categories. Further, a change in ECG category during a measurement was frequently, but not always, found to be simultaneous with a change in the rotation pattern of the MFO. Utilization of spatial information of MCG mapping could enable detection of both regularities and instantaneous phenomena during AF. *Significance*: Cardiac mapping may offer a useful noninvasive means to study the mechanisms of AF, including superior temporal resolution.

1. Introduction

Atrial fibrillation (AF) is characterized by disorganized electrical activity in the atria. This activity is, however, not entirely random (Gerstenfeld *et al* 1992) but shows a dynamically changing activation pattern with various degrees of local spatial organization (Konings *et al* 1994, Lee *et al* 2014). The complexity of the electrical activity has been linked to the persistence of AF (Allessie *et al* 2010, Lee *et al* 2014) and the predictability of treatment outcome (Yoshida *et al* 2012, Meo *et al* 2013).

Direct invasive study is considered to be the gold standard in assessing atrial activity, but it can be performed only during electrophysiological study or open heart surgery, so limiting the wide application of such mappings. The characterization of AF from body-surface electrocardiograms (ECGs) has received attention in recent years (Lankveld *et al* 2014). Such approaches would seem to offer the means to obtain information in a noninvasive manner on the complexity of AF and could be useful in the planning of therapy. Most studies used a traditional 12-lead ECG. There is emerging evidence, however, that expanding the spatial coverage by using multiple leads may increase the performance (Meo *et al* 2013), and that an additional posterior lead or leads may provide more information on the left atrial activity (Guillem *et al* 2013). For maximal spatial information, body-surface

© 2018 Institute of Physics and Engineering in Medicine

potential mapping (BSPM) has been proposed, with tens of electrodes covering the thorax and indeed, surface potential distribution has been shown to reflect the spatial distribution of AF activity (Cuculich *et al* 2010, Guillem *et al* 2009, 2013, Lankveld *et al* 2014).

The electrical activity of the heart gives rise to an electromagnetic field. Complementing ECGs and BSPM, magnetocardiography (MCG) and MCG mapping provide data on the magnetic field time development and its spatial distribution, i.e. the so-called MCG map pattern, through multichannel measurement near the subject's chest without physical contact. Although MCG has been applied to the study of several heart diseases (Kwong *et al* 2013), only a few studies have assessed ongoing AF (Kim *et al* 2007, Nakai *et al* 2008, Yoshida *et al* 2012). In particular, the dynamic properties of MCG signal spatial patterns during ongoing AF have so far not been published.

In this study, we demonstrate the temporal evolution of MCG map patterns during ongoing AF. To describe the recurrent patterns observed, a simple dimension reduction method of multichannel MCG data is applied. We present the possibility of quantifying the temporal evolution of MCG map patterns during AF with the method and potential of the MCG in the characterization of AF in general. Furthermore, we study the relationship between spatiotemporal MCG patterns and variation in ECG waveform during AF.

2. Materials and methods

2.1. Patients and MCG measurements

In this study, nine patients with AF and one patient with common (counter-clockwise) atrial flutter were chosen to represent typical, clinically classical atrial arrhythmias. Four of the patients were diagnosed with hypertension and two with dilated cardiomyopathy. Five of the patients had AF without any other underlying cardiac disease (lone AF). All the patients were treated in the Helsinki University Hospital, and signed informed consent was obtained from all subjects. The study was approved by the Ethical Review Board of the institute.

The MCG instrumentation has been described comprehensively (Jurkko *et al* 2009). Briefly, the magnetocardiograms were recorded in a magnetically shielded room (ETS-Lindgren Euroshield Oy, Eura, Finland) with a 99-channel cardiomagnetometer (Neuromag, Helsinki, Finland). For each measurement, the center of the sensor array was positioned over the anterior chest, 15 cm below the jugular notch and 5 cm to the left of the midsternal line. Each measurement continued for at least 7 min (421–902 s) during arrhythmia, and simultaneously with the MCG, the limb leads of the standard ECG and bipolar *XYZ* leads were recorded. The analog signal pass-band was 0.03–300 Hz and analog-to-digital sampling frequency was 1 kHz.

2.2. MCG signal preprocessing and atrial signal extraction

To confine the MCG analysis to atrial activity, TQ intervals were extracted; we refer to these as 'AF intervals'. First, the QRS complexes were detected using a correlation technique with a manually selected template waveform on three ECG channels. When necessary, more than one template was used. Then, for each recording, the QRST time interval was determined utilizing superimposed complexes, and also signal averages on all ECG and MCG channels. No appreciable ventricular signal was allowed during the AF intervals. Segments of data containing excessive noise (e.g. due to movement) were identified and excluded. Finally, only those AF intervals having durations of at least 250 ms were selected for further analysis. The data browsing and preprocessing was performed using in-house software[4].

The recordings were carefully preprocessed, to remove noise while preserving the original atrial signal. The signal space projection (SSP) method was used to reduce external interference (Uusitalo and Ilmoniemi 1997). To remove baseline wander, a high-pass Butterworth filter was specified, with a 2–4 Hz transition band and 12 dB stop-band rejection, allowing 1 dB pass-band ripple. In addition, a low-pass filter with a 120–150 Hz transition band was used. For minimal filter ringing, before filtering the specified AF intervals were joined by linear interpolation over the time intervals of excluded ventricular activity, using a Hanning window weighting function to smoothen the ends of the AF intervals. To avoid phase distortion, all the filters were run bi-directionally. The signal processing was performed using Matlab[5]. Figure 1(a) shows one extracted and filtered AF interval on 33 magnetometer locations.

2.3. Magnetic field map visualization and characterization

We used pseudo current conversion (Cohen and Hosaka 1976) to visualize and characterize the MCG mappings, as previously described (Jurkko *et al* 2009). Briefly, the distribution of magnetic field component B_z was reconstructed on the sensor array surface. This distribution was visualized as an isofield map (for example, see figure 1(b)) and used to construct a so-called pseudo current density (PCD) map:

[4] Canalyse, Heikki.Vaananen@aalto.fi
[5] www.mathworks.com

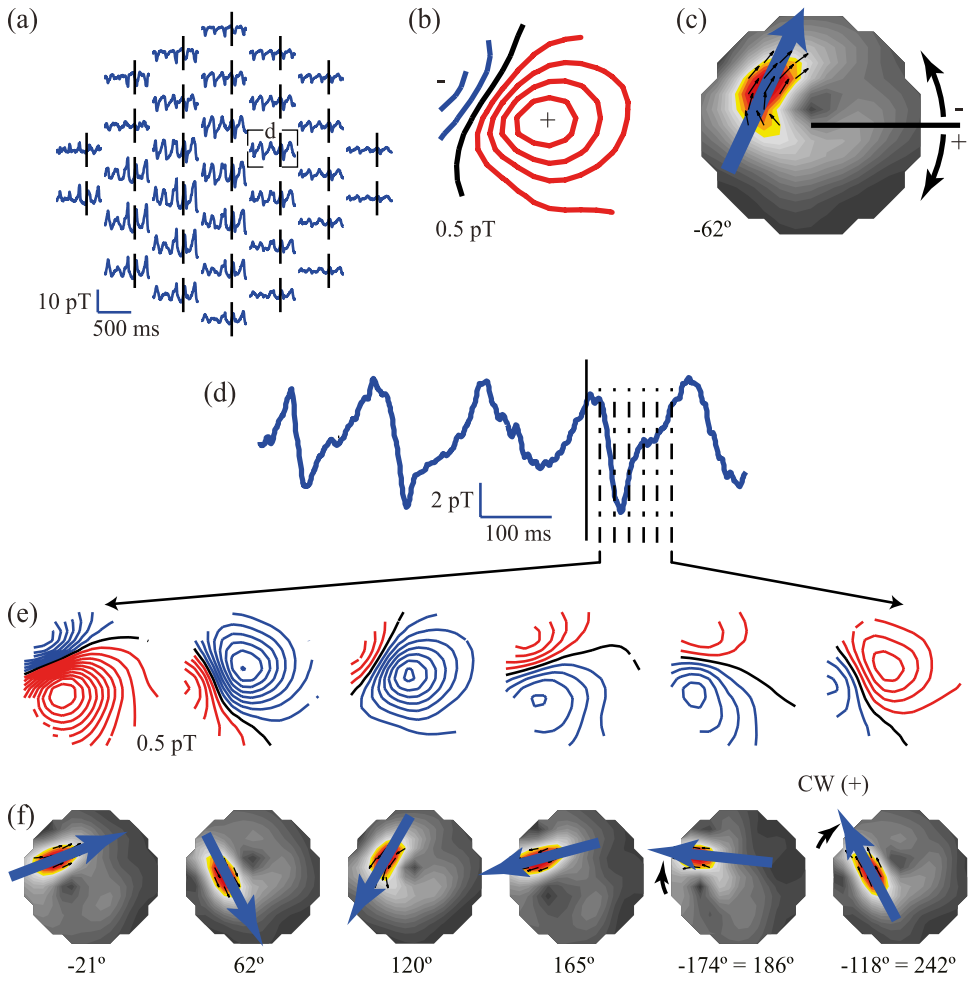

Figure 1. Atrial fibrillation (AF) signal in MCG and magnetic field map orientation (MFO). (a) Preprocessed AF signals in 33 magnetometers over one AF interval. (b) Isocontours of the magnetic field. The blue color (−) indicates flux out of the chest and the red color (+) into the chest; the step between adjacent lines is 0.5 pT. (c) Pseudo current density (PCD) map and MFO; the amplitude is shown using false color-coding scaled to the maximum; the orientations of the strongest pseudo current vectors (the yellow–red area) are shown with black arrows and their mean orientation is defined as the MFO, shown below the plot and illustrated with the thick blue arrow. (Length is not related to amplitude.) The time instant of maps (b) and (c) is indicated over the signals in (a) with black vertical bars. The zero angle of direction in (c) (black horizontal line) is pointing from subject's right to left, and positive direction of rotation is clockwise (CW). (d) MCG waveform of one channel; the sequence of (e) isofield and (f) the corresponding PCD maps show CW rotation with time. Here, the smallest angle between successive MFOs is always positive (CW direction, black curved arrows), resulting in an increasing angle of MFO in terms of nearest 360° complements. The sequence follows in time the maps presented in (b) and (c) at 20 ms intervals; the time instants are indicated in (d) with vertical dashed bars. For further explanation, see text.

$$\vec{a} = \frac{\partial B_z}{\partial y}\hat{e}_x - \frac{\partial B_z}{\partial x}\hat{e}_y,$$

where $\hat{e}_x$ and $\hat{e}_y$ are the perpendicular unit vectors on the sensor array plane. Figure 1(c) shows the PCD map corresponding to the isofield map in figure 1(b). The magnetic field map orientation (MFO, in degrees of angle) was defined as the mean orientation of the top 30 percent of the strongest pseudo current vectors, as illustrated in figure 1(c) (Jurkko *et al* 2009). This kind of distribution-based estimate is more robust than, for example, that corresponding to the maximum gradient of B_z (Cohen and Hosaka 1976), and also enables a reliability assessment to be made of each MFO value, using circular statistics. Using Rayleigh's test (Zar 1999), only statistically significant mean orientations ($p < 0.01$) were accepted for further analysis. In addition, mean amplitude was determined from this same distribution and only those MFOs corresponding to maps exceeding a baseline noise level of 7 pT m^{-1} were accepted. This noise level was set at the 99th percentile of noise amplitude, determined by applying the analysis on two measurements made with the MCG system in the shielded room without a patient.

To investigate the dynamics of AF, we constructed PCD map animations over the AF intervals. First, the maps were created for every sample, i.e. at every millisecond. Then, the maps were created also using a 20 ms moving average at every 5 ms; this also reduced any remaining noise after preprocessing. Figure 1 shows an example of a

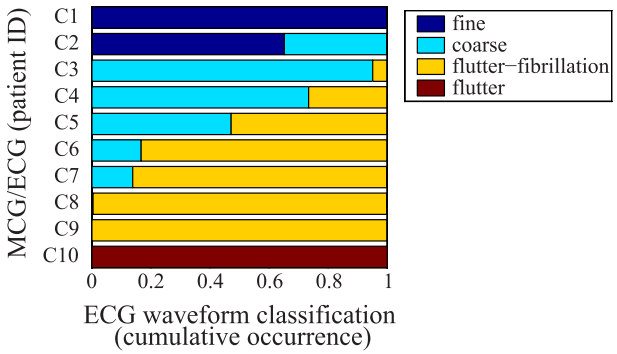

Figure 2. Cumulative occurrences of the four categories of atrial arrhythmia in ECG. For each patient, cumulative occurrence over the recording is shown by a stacked horizontal bar in the defined colors. For further explanation, see text.

sequence of maps (at 20 ms intervals for illustrative purposes). Here the maps and the MFO have an appearance of clockwise (CW) rotation with time. The series of maps over all AF intervals included were joined and reviewed as animations as well as inspected in terms of the MFO.

As orientation is a circular variable, the MFO is always within a range of 360°, here between −180 and +180°. We plotted the MFO as a function of time while taking its circularity into account. Each new value of the MFO in the time sequence was replaced by its 360° complement nearest to the previous value (Matlab function *unwrap*). This is illustrated in figure 1(f). When this transformed sequence is plotted against time, the CW rotation of the MFO appears as an upward slope whereas counter-clockwise (CCW) rotation results in a downward slope. This kind of plot clearly shows changes in the direction of the rotation, and the magnitude can also be interpreted as cumulative rotation.

2.4. Simultaneously recorded ECG waveform for comparisons

While there is no generally accepted classification for different ECG waveforms of AF, the AF signal is commonly described as either fine or coarse, based on its amplitude and regularity (for example, see Gallagher and Camm (1998)). Moreover, the latter with a relatively regular pattern has also been called flutter-fibrillation. We applied these descriptions to create a customized classification scheme. The ECG recorded simultaneously with the MCG was inspected by a cardiologist (M.L.) who was unaware of the MCG analyses. He used custom-made software to classify distinguishable segments of the recordings into four categories, with the following criteria: the arrhythmia was considered (1) *fine fibrillation* when at least seven of the nine ECG leads showed fine fibrillatory signals by visual evaluation, with amplitudes of less than 50 μV; (2) *coarse fibrillation* when three or more leads showed fibrillatory wave amplitudes of at least 50 μV; (3) *flutter-fibrillation* when coarse fibrillation segments were perceived to carry a relatively regular pattern, still allowing irregular waveform in some leads, and; (4) *atrial flutter* when a regular temporal pattern with a rate in the range of 250–350 per minute was observed in all leads.

3. Results

3.1. AF intervals and ECG description

The mean duration of the AF intervals per recording ranged from 418 ms to 691 ms. The cumulative duration of all the intervals analyzed ranged from 30 percent to 59 percent of the total duration of each recording for the cases presenting AF in the ECG (recordings C1–C9). The flutter recording (C10) showed acceptable length (>250 ms) arrhythmia intervals of only 5 percent of the total duration due to a high ventricular rate.

The ECG classification results are summarized in figure 2 and table 1. Note that, unlike for the 'pure' AF intervals described above, segments of recordings here also include QRST intervals within them. For the presentation of the data in this paper, the recordings were manually ordered and numbered based on the ECG waveform classification.

3.2. Magnetic field map animation and orientation time course

In MCG map animations, both organized as well as irregular spatiotemporal patterns were observed. In general, the time evolution of the maps was found to be continuous and smooth. Recurrent spatiotemporal patterns were observed in all patients. The strongest PCD vectors were concentrated in the region approximately above the atria and were usually confined to a single area with coherent orientation, enabling intuitive interpretation of the magnetic field map orientation (for example, see figure 1). In the animations, rotation of the maps and sudden changes in the direction of the rotation were frequent.

Table 1. Summary of the ECG waveform classification and arrhythmia segment statistics. No sinus rhythm was detected during the recordings. The patients were ordered such that the identification number increased with the level of supposed organization in the atrial activity.

Recording		Fine fibrillation		Coarse fibrillation		Flutter-fibrillation		Atrial flutter	
ID	Dur.[a]	*N*[b]	Duration[c]	*N*	Duration	*N*	Duration	*N*	Duration
C1	421	1	417.4 ± 0.0						
C2	433	17	16.6 ± 14.7	17	8.9 ± 3.9				
C3	624			8	74.0 ± 140.5	7	4.4 ± 2.5		
C4	421			23	13.4 ± 10.7	24	4.6 ± 3.0		
C5	517			25	9.7 ± 9.3	25	10.9 ± 11.8		
C6	440			15	4.9 ± 3.2	16	22.8 ± 21.0		
C7	902			25	5.0 ± 2.6	25	31.0 ± 24.8		
C8	421			1	1.6 ± 0.0	2	208.6 ± 245.9		
C9	591					1	589.2 ± 0.0		
C10	421							1	419.3 ± 0.0

[a] Duration of recording in seconds.
[b] Number of segments.
[c] Arrhythmia segment duration mean ± SD in seconds.

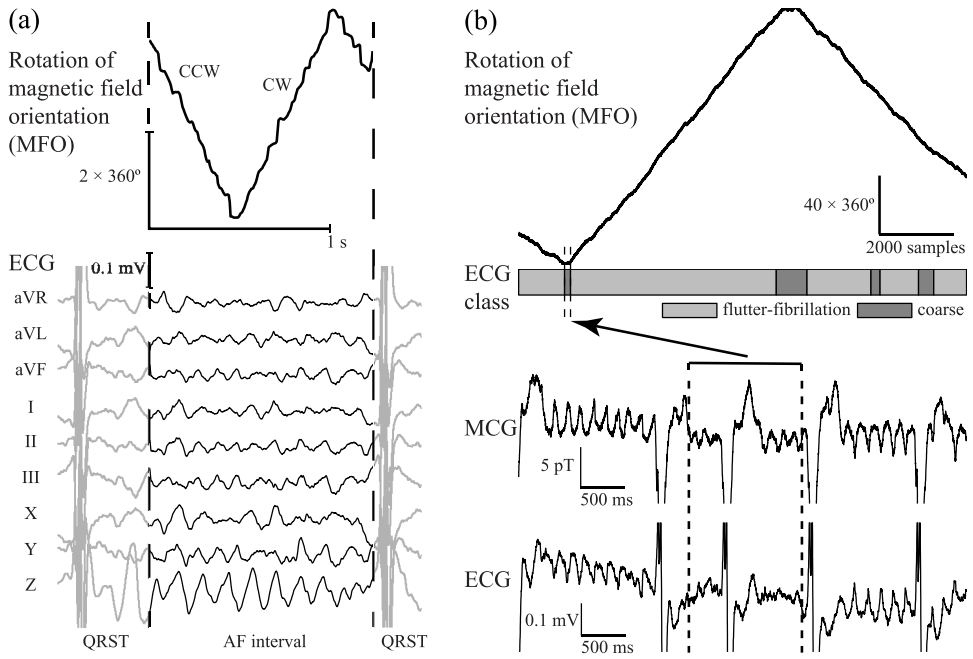

Figure 3. Time course of the MFO and the concurrent ECG. (a) MFO and ECG are shown over one AF interval during AF in patient C3. In the MFO plot (upper panel), the descending parts indicate counter-clockwise (CCW) and the ascending part clockwise (CW) rotation of the MFO with time. Here the rotation changes direction twice within a single AF interval. The concurrent ECG (lower panel), was classified as flutter-fibrillation for the whole period shown. The vertical scale bar in the upper panel indicates rotation corresponding to two full 360° cycles (zero angle arbitrary), and, in the lower panel, the ECG amplitude. The timescale is identical in the two panels and is shown with the horizontal bar. (b) MFO and the ECG classification (upper panel) are shown over several consecutive AF intervals in patient C7. The two changes in the direction of rotation of the MFO co-occur with the first two segments of coarse AF in ECG, but during the following two segments of coarse AF there is no change in rotation. MCG and ECG waveforms (lower panel), including the first segment of coarse AF, seem to change in polarity. The MFO and the ECG classification (upper panel) are plotted in the same timescale over a period of about 2 min of the recording. The timescale is shown with a horizontal bar and indicated in samples, with the typical sample-to-sample interval being 5 ms. The timescales of MCG and ECG waveforms (lower panel) are identical and are shown below the waveforms. For more details, see text and supplementary animations 1 and 2 online (stacks.iop.org/PM/39/025006/mmedia) corresponding to *A* and *B*, respectively.

The quantification of magnetic field map orientation, MFO, corresponded well to the visually perceived patterns. Thus, rotation appeared as a slope when plotting the MFO against time, as explained earlier. As an example, an MFO plot over one AF interval in case C3 is shown in figure 3(a). During the first half (of a second) in the figure, the descending slope corresponds to the counter-clockwise (CCW) rotation. At about 0.5 s from the beginning, it changes abruptly and becomes an ascending slope, because of the change from CCW into CW rotation of the MFO. See also the corresponding supplementary animation 1 online (stacks.iop.org/PM/39/025006/mmedia).

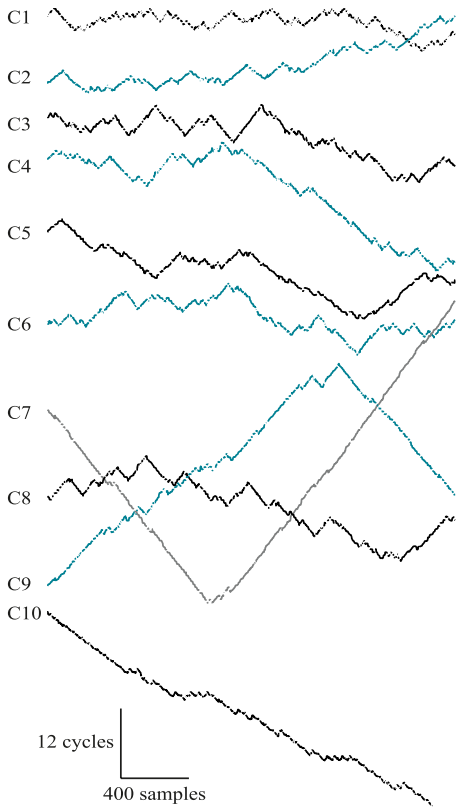

Figure 4. Time course of the MFO. Example of the MFO plot in each patient of this study. Patients have been ordered according to the supposed level of organization of atrial activity, as described in the text. (See also figure 2 and table 1.) The blank (white) areas in the plots correspond to samples where the magnetic field map did not have a clear orientation or the signal amplitude was below the noise level. Note that colors are used only to aid separation of the plot of each case from the others. For further explanation, see text and figure 1.

The persistence of rotation and its direction were found to vary not only between cases but also during recording. In figure 3(b) (upper panel), the MFO plot over several AF intervals during about 2 min of the recording is shown for case C7. Here, the rotation and its direction, in particular, are clearly more persistent in comparison to the previous example (figure 3(a)). In figure 3(b) the MFO is shown only for the AF intervals, i.e. the QRST intervals have been omitted, as explained earlier. See also supplementary animation 2 online (stacks.iop.org/PM/39/025006/mmedia).

An example of an MFO plot for each patient in this study is shown in figure 4. Each plot consists of 2400 consecutive orientation samples (at 5 ms intervals). On average, this corresponds to 25 s of measurement time (range 20–36 s) consisting of 21 AF intervals (range 16–32) for cases C1–C9. The plot for patient C10 with atrial flutter corresponds to about 329 s of measurement time with 26 AF intervals, due to a high ventricular rate. When the MFO could not be reliably determined, there is a blank. In the figure, the slopes in the MFO plots appear with variable duration and orientation, positive (CW) and negative (CCW), indicating both the regularity and variation observed in the MCG mappings of AF.

3.3. Comparison with ECG categories

A change of character in the MCG map time evolution, in the rotation pattern of the MFO in particular, was frequently but not always associated with a change in ECG. The example in figure 3(a) shows that the rotation of the MFO may abruptly change direction without a clear change in the concurrent ECG. At times, a change of character in the MCG maps co-occurred with a change in the ECG category. Such a case is illustrated in figure 3(b) where at first a fairly consistent CCW rotation (a downward slope in the MFO plot) spanning several AF intervals was observed during flutter-fibrillation in the ECG, and then, with a short segment of coarse fibrillation in the ECG, the MCG maps showed smooth but irregular time behavior with rather constant MFO. Further, in this case, coincident with the return of flutter-fibrillation in the ECG, the direction of rotation was inverted to CW (sloping upwards). In this case, the direction of rotation was associated with distinct MCG and ECG waveforms in some channels, as shown in the lower panel of figure 3(b). Still for the same case, with the second segment of coarse fibrillation, the direction of rotation was inverted again to CCW (downward sloping), but the last two segments of coarse fibrillation, on the other hand, were not associated with a change in rotation. Instead, the CCW rotation seemed to persist.

Rotation of the MFO could be observed with all patients and was not constricted by either the ECG category or the ordering. In figure 4, the plots have been ordered based on the ECG classification results summarized in figure 2 and table 1, assuming increasing regularity top-down. In cases C1–C6 there are relatively short segments of MFO with a slope; in the animations, rotation was observed only occasionally. Especially in case C1, with fine fibrillation in the ECG, it is relatively frequent that MFO could not be determined reliably, indicating not only complex MCG map patterns but also low MCG amplitude. See also supplementary animation 3 online (stacks.iop.org/PM/39/025006/mmedia), depicting case C2 with fine fibrillation in the ECG. In cases C7–C9, on the other hand, the MFO can mostly be determined and forms mostly slopes; in the animations, these cases showed clear rotation. Case C10 with atrial flutter showed consistent CCW rotation. This rotation in general seemed to be slower compared to the other patients with AF, as indicated by the MFO plot with its less steep slope.

3.4. Magnetic field map orientation time course—analysis example

As an example of how to quantify the temporal features of an MCG map pattern using its orientation, we propose three metrics computed from the MFO time course, concentrating on the rotation. Here we define rotation as being *consistent* when the MFO time course shows a clear slope over at least one full cycle, as in figure 3, for example. To detect the time intervals with consistent rotation, we fitted[6] a piecewise linear polynomial function to the MFO time course; this was done separately on each AF interval. The number of cycles of rotation in either direction within these (rotation) intervals can then be quantified as, for example, the *rotation sum*. As shown in figure 3, the direction of rotation may change abruptly or it may persist. To quantify this, we define *recurrence* as an event with consistent rotation in either direction followed by consistent rotation in the same direction in the next detected rotation interval; in between these two parts, the MFO is allowed to show no rotation, for example because of a QRS complex. Similarly, *reversal* of rotation is defined as an event with consistent rotation in either direction, followed by consistent rotation in the other direction.

Figure 5 shows the rotation sum and the number of recurrence and reversal events in the MFO plots in figure 4; the rotation sum and the number of recurrence events are shown separately for CW and CCW directions. In this, the consistent rotation intervals with the slope of the fit of < 15 cycles per second were counted. Visually, the heights of the bars expressing the number of events/cycles correspond well with the MFO plots in figure 4. Exact manual counting of the events/cycles from figure 4 is difficult, even though it covers only about 25 s of measurement time.

4. Discussion

In this study, we visualized MCG maps of the ongoing AF as animations. Further, we plotted the time course of magnetic field map orientation (MFO). In the animations, we observed spatial organization and temporally smooth sequences, together often perceived as rotation of the map. This rotation, as well as its sudden changes in direction, was also apparent in the time course of the corresponding MFO. These novel findings are most likely reflections of fibrillatory activity. Our results thus suggest that the spatial information of a noninvasive multichannel measurement, such as MCG, can be used to detect instantaneous and sudden fibrillatory phenomena in almost real-time. As the short-time dynamics of AF are largely unexplored, at least noninvasively, this kind of information has the potential to advance our understanding of the disease. The information also clearly has the potential to be diagnostically useful and it could eventually have implications on treatment as well.

The ECG recorded simultaneously with the MCG was used for comparisons. Because a generally accepted classification for the ECG waveform of AF is still lacking, a robust custom scheme was created to describe the recordings based on waveform amplitude and regularity. Although only 10 patients were studied, a representative coverage of fibrillatory signals was detected in the ECG. The results show that rotation of the MFO could be observed in all the patients under study, and in each ECG category. Considerable variability in the emergence and persistence of the rotation was observed, as well as in its direction, but the rotation of the MFO in general was found to be more persistent in patients with more organized atrial activity in the ECG. Temporal correspondence between changes in the MCG-based rotation of MFO and changes between the signal categories in the ECG was found to be only partial. In a further comparison, the frontal angle of the so-called heart vector computed from ECG (data not shown) showed orientation and time course similar to MFO, but the two did not always correlate, i.e. they showed different rotations with time. This suggests that, referring to ECG, MCG may provide both supplementary and complementary information on electrical activity during AF.

[6] Using Matlab toolbox 'SLM—shape language modeling' by John D'Errico. https://se.mathworks.com/matlabcentral/fileexchange/24443-slm-shape-language-modeling

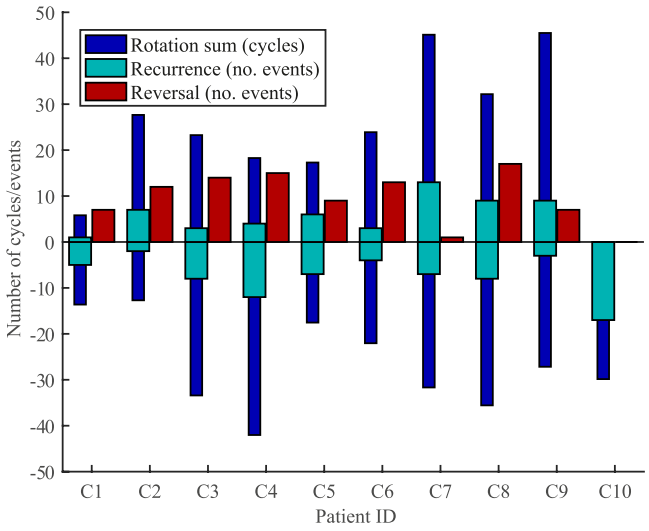

Figure 5. An example of quantifying rotation of MFO, applied on the plots in figure 4. When the MFO time course shows an interval with a clear slope over at least one full cycle (as in figure 3(a), for example), rotation is considered to be *consistent* and is taken into account. When two consecutive rotation intervals show rotation in the same direction (i.e. CW or CCW) it is called an event of *recurrence*, whereas when the direction changes, this is called an event of *reversal*. The sum of cycles of consistent rotation (*rotation sum*) and the number of recurrence and reversal events are shown for each patient, with vertical bars. For the sum and recurrence events, cycles and events are shown separately for CW and CCW rotation as positive and negative, respectively. For detailed explanation, see text.

4.1. Magnetocardiographic mapping of atrial fibrillation

Prior to the current study it was not known how the possible organization and dynamics of atrial activity during AF would appear in MCG. In their study on atrial flutter, Yamada *et al* described the PCD patterns of AF as disorganized (Yamada *et al* 2003). However, only brief segments of AF were reported, related to the onset of atrial flutter. In line with those findings, the AF in our animations also appears to be disorganized at times. Obviously, MFO is only one approach to the characterization of MCG mapping; other good approaches may exist. We mainly studied the MFO time course, and it is possible that characteristic spatial patterns that could perhaps be linked to certain AF processes may exist. Such an association was suggested by Guillem *et al* using BSPM (Guillem *et al* 2009). Consistent with our findings, they reported inter-individual differences and also rotation of the BSPM pattern, but they did not report a temporal relationship between the patterns.

MCG measures the magnetic field generated by the same electrochemical activity of the heart that gives rise to the ECG. The sensitivity of MCG to detect cardiac activity is, however, complementary in nature in comparison to ECG/BSPM (Wikswo 1983, Mäntynen *et al* 2014). It is likely that MCG can discern some part of the atrial activity better than ECG/BSPM. In the atria, most of the activity spreads tangentially because the walls are thin and MCG is relatively more sensitive to tangential source currents (Wikswo 1983, Mäntynen *et al* 2014), whereas the ECG signal may be attenuated. Moreover, spatially fractionated activity with multiple wavelets during AF (Konings *et al* 1994, Allessie *et al* 2010, Lee *et al* 2014) may even appear as partial current loops with a weak ECG but a relatively strong MCG signal (Liehr *et al* 2005).

Unlike AF, typical atrial flutter is relatively well described (SippensGroenewegen *et al* 2000, Yamada *et al* 2003). Using MCG, Yamada *et al* reported a circular PCD pattern with counter-clockwise curvature during atrial flutter (Yamada *et al* 2003). In the instantaneous maps of our animation, we observed not only a very similar pattern but also patterns with clockwise curvature (data not shown). This can likely be explained by the differences of sensor arrays and their positioning. Despite this, the direction of rotation of MFO *with time* was consistently counter-clockwise, which is also consistent with the rotation of the BSPM pattern as presented by SippensGroenewegen *et al* (2000).

4.2. Mapping facilitates detection of instantaneous phenomena in AF

Invasive studies have described transient spatial organization of activity that consists of a few repetitions of similar activation patterns (Gerstenfeld *et al* 1992, Konings *et al* 1994, Allessie *et al* 2010, Lee *et al* 2014). The duration of these transient segments can be as short as two cycles, or a couple of hundred milliseconds in time, and often less than a second. Still, such short-time dynamics of AF are largely unexplored, at least noninvasively; ECG-based measures to characterize AF have typically been constructed using signal segments lasting for 10 s (Lankveld *et al* 2014). While such global measures are promising, for example in the prediction of rhythm control therapy outcome (Lankveld *et al* 2014), the information they carry about the possible short-time dynamics of AF within a segment is blurred (Alcaraz *et al* 2012). Recently, Haissaguerre *et al* (2014) reported continuously

changing activation wavefronts and spatially meandering 'AF driver domains', estimated by solving the inverse problem using multichannel ECGs with individual atrial and thorax models.

By condensing multichannel data over a short sampling interval into a single metric, it is possible to detect and quantify instantaneous phenomena in the time course of the feature that the metric describes. As the MFO in this study is determined from spatial information for each short time interval separately, it provides an almost instantaneous global measure of the prevailing electrical activity. Our results show that changes in rotation of the MFO occur suddenly, with timing similar to that found in invasive mappings. This suggests that at least some of the abrupt changes in the atrial electrical activity can also be detected noninvasively, without extensive (inverse) modelling. Inverse modelling, such as in Haissaguerre *et al* (2014), could be applied to MCG for estimating the atrial activation patterns in a manner similar to recent BSPM studies (e.g. Cuculich *et al* (2010) and Haissaguerre *et al* (2014)). Such approaches, however, demand accurate geometrical models and constraints on the solution, in order to obtain usable estimates from the ill-posed inverse problem. In practice, anatomical imaging, such as a computed tomography scan, and prior assumptions about a certain kind of activity are needed. To the contrary, the present sensor-level approach is relatively model-free, with minimal prior assumptions about the atrial activity. In addition, MCG is totally contactless and the measurement can be done relatively quickly, making it feasible for screening purposes, for example.

With the limited number of patients in this study, a clinically meaningful further analysis of the MFO plots, and their transient features in particular, is outside the scope of this work. The analysis shows, however, that the approach should be applicable to a wide range of AF signals. Because the recording of an invasive reference simultaneously with MCG is very difficult, if not impossible, the value of our observations and approach to quantify them should be evaluated, for example in a group of patients assigned to catheter ablation for treatment of AF.

The sequences of recurrent rotation and abrupt reversals in its direction could be detected with a time resolution well below one second; invasive studies have described transient spatial organization with a very similar temporal behaviour (e.g. Lee *et al* (2014)). The angular velocity of MFO (rotation) likely describes a signal feature related to the body-surface main/dominant frequency of AF, judging by the values (not shown) agreeing with those reported for MCG (Yoshida *et al* 2015). In case of the MFO, however, the 'frequency' can be estimated from just a few rotations to within a couple of hundred milliseconds. Whether these or some other derived metrics have clinical value remains to be studied. It seems plausible that the capability to detect dynamics in fibrillatory activity, perhaps in combination with fibrillatory-wave morphology assessment, can open a new perspective for noninvasive study of AF.

5. Conclusions

This is the first study to systematically assess the temporal evolution of magnetocardiographic (MCG) map patterns during ongoing atrial fibrillation (AF). The MCG mapping of ongoing AF shows transient organization and recurrent time behavior that can be characterized in high time resolution. This study suggests that noninvasive mapping such as MCG might enable the detection of instantaneous phenomena during AF through the application of increased spatial information. Consequently, noninvasive mapping methods may offer the means to study the mechanisms of AF with high temporal resolution, and the increased spatiotemporal information may advance our understanding of the disease. The real advantage gained by the use of magnetocardiography, the here reported finding of the recurrent patterns, and the here documented approach can be found out in separate studies, possibly in combination with ECG, with proper populations of AF patients.

Acknowledgments

We gratefully thank Lic. Sc. (Tech.) Heikki Väänänen for technical support on the cardiac signal analysis software. This work was funded by the Finnish Foundation for Cardiovascular Research; the Aalto University School of Science and Technology; the Academy of Finland (141102); and Helsinki University Hospital District research funds (EVO), grant number TYH2015120.

ORCID iDs

Ville Mäntynen https://orcid.org/0000-0002-6121-0090
Mika Lehto https://orcid.org/0000-0002-8691-5142

References

Alcaraz R, Hornero F, Martínez A and Rieta J J 2012 Short-time regularity assessment of fibrillatory waves from the surface ECG in atrial fibrillation *Physiol. Meas.* **33** 969–84

Allessie M A, de Groot N M S, Houben R P M, Schotten U, Boersma E, Smeets J L and Crijns H J 2010 Electropathological substrate of long-standing persistent atrial fibrillation in patients with structural heart disease: longitudinal dissociation *Circ. Arrhythm. Electrophysiol.* **3** 606–15

Cohen D and Hosaka H 1976 Part II magnetic field produced by a current dipole *J. Electrocardiol.* **9** 409–17

Cuculich P S, Wang Y, Lindsay B D, Faddis M N, Schuessler R B, Damiano R J, Li L and Rudy Y 2010 Noninvasive characterization of epicardial activation in humans with diverse atrial fibrillation patterns *Circulation* **122** 1364–72

Gallagher M M and Camm J 1998 Classification of atrial fibrillation *Am. J. Cardiol.* **82** 18N–28N

Gerstenfeld E P, Sahakian A V and Swiryn S 1992 Evidence for transient linking of atrial excitation during atrial fibrillation in humans *Circulation* **86** 375–82

Guillem M S, Climent A M, Castells F, Husser D, Millet J, Arya A, Piorkowski C and Bollmann A 2009 Noninvasive mapping of human atrial fibrillation *J. Cardiovasc. Electrophysiol.* **20** 507–13

Guillem M S, Climent A M, Millet J, Arenal Á, Fernández-Avilés F, Jalife J, Atienza F and Berenfeld O 2013 Noninvasive localization of maximal frequency sites of atrial fibrillation by body surface potential mapping *Circ. Arrhythm. Electrophysiol.* **6** 294–301

Haissaguerre M *et al* 2014 Driver domains in persistent atrial fibrillation *Circulation* **130** 530–8

Jurkko R, Mäntynen V, Tapanainen J M, Montonen J, Väänänen H, Parikka H and Toivonen L 2009 Non-invasive detection of conduction pathways to left atrium using magnetocardiography: validation by intra-cardiac electroanatomic mapping *EP Eur.* **11** 169–77

Kim D, Kim K, Lee Y-H and Ahn H 2007 Detection of atrial arrhythmia in superconducting quantum interference device magnetocardiography; preliminary result of a totally noninvasive localization method for atrial current mapping *Interact. Cardiovasc. Thorac. Surg.* **6** 274–9

Konings K T, Kirchhof C J, Smeets J R, Wellens H J, Penn O C and Allessie M A 1994 High-density mapping of electrically induced atrial fibrillation in humans *Circulation* **89** 1665–80

Kwong J S W, Leithäuser B, Park J-W and Yu C-M 2013 Diagnostic value of magnetocardiography in coronary artery disease and cardiac arrhythmias: a review of clinical data *Int. J. Cardiol.* **167** 1835–42

Lankveld T A R, Zeemering S, Crijns H J G M and Schotten U 2014 The ECG as a tool to determine atrial fibrillation complexity *Heart* **100** 1077–84

Lee G *et al* 2014 Epicardial wave mapping in human long-lasting persistent atrial fibrillation: transient rotational circuits, complex wavefronts, and disorganized activity *Eur. Heart J.* **35** 86–97

Liehr M, Haueisen J, Goernig M, Seidel P, Nenonen J and Katila T 2005 Vortex shaped current sources in a physical torso phantom *Ann. Biomed. Eng.* **33** 240–7

Mäntynen V, Konttila T and Stenroos M 2014 Investigations of sensitivity and resolution of ECG and MCG in a realistically shaped thorax model *Phys. Med. Biol.* **59** 7141–58

Meo M, Zarzoso V, Meste O, Latcu D G and Saoudi N 2013 Spatial variability of the 12-lead surface ECG as a tool for noninvasive prediction of catheter ablation outcome in persistent atrial fibrillation *IEEE Trans. Biomed. Eng.* **60** 20–7

Nakai K, Oka T, Okabayashi H, Tsuboi J, Fukuhiro Y, Fukushima A, Suwabe A, Itoh M and Yoshizawa M 2008 Three-dimensional spectral map of atrial fibrillation by a 64-channel magnetocardiogram *J. Electrocardiol.* **41** 123–30

SippensGroenewegen A, Lesh M D, Roithinger F X, Ellis W S, Steiner P R, Saxon L A, Lee R J and Scheinman M M 2000 Body surface mapping of counterclockwise and clockwise typical atrial flutter: a comparative analysis with endocardial activation sequence mapping *J. Am. Coll. Cardiol.* **35** 1276–87

Uusitalo M A and Ilmoniemi R J 1997 Signal-space projection method for separating MEG or EEG into components *Med. Biol. Eng. Comput.* **35** 135–40

Wikswo J P Jr 1983 Theoretical aspects of the ECG-MCG relationship *Biomagnetism: an Interdisciplinary Approach* ed S J Williamson *et al* (New York: Plenum) pp 311–26

Yamada S, Tsukada K, Miyashita T, Kuga K and Yamaguchi I 2003 Noninvasive, direct visualization of macro-reentrant circuits by using magnetocardiograms: initiation and persistence of atrial flutter *Europace* **5** 343–50

Yoshida K, Ogata K, Inaba T, Nakazawa Y, Ito Y, Yamaguchi I, Kandori A and Aonuma K 2015 Ability of magnetocardiography to detect regional dominant frequencies of atrial fibrillation *J. Arrhythmia* **31** 345–51

Yoshida K *et al* 2012 Electrogram organization predicts left atrial reverse remodeling after the restoration of sinus rhythm by catheter ablation in patients with persistent atrial fibrillation *Heart Rhythm* **9** 1769–78

Zar J H 1999 *Biostatistical Analysis* (Upper Saddle River, NJ: Prentice-Hall)